Microstructural Characterization of Rapidly Solidified Al-High Si Alloys

4 authors:

H. V. Atkinson
University of Leicester
147 PUBLICATIONS **3,474** CITATIONS

SEE PROFILE

F. Alshmri
Prince Sattam bin Abdulaziz University
8 PUBLICATIONS **13** CITATIONS

SEE PROFILE

Sarah V Hainsworth
University of Leicester
85 PUBLICATIONS **1,548** CITATIONS

SEE PROFILE

S.D.A. Lawes
University of Nottingham
19 PUBLICATIONS **107** CITATIONS

SEE PROFILE

Microstructural Characterization of Rapidly Solidified Al-High Si Alloys

H.V. Atkinson[1, a], F. Alshmri[2, b], S.V. Hainsworth[1, c] and S.D.A. Lawes[1, d]

[1]Department of Engineering, University Road, Leicester, LE1 7RH, UK

[2]Formerly of the Department of Engineering, University Rd., Leicester, LE1 7RH, UK, now of   P.O. Box 59874, Riyadh11535, Saudi Arabia

[a]hva2@le.ac.uk, [b]eng_fraj@hotmail.com, [c] svh2@le.ac.uk, [d] sdal1@le.ac.uk

Abstract. Aluminium silicon alloys are the most used raw material for automotive applications. One of the main limitations on using aluminium *high* silicon alloys is the formation of coarse brittle phases under conventional solidification conditions. However, rapid solidification processing (RS) (for example, through melt spinning) is very effective in limiting the coarsening of primary silicon due to the high cooling rate. In the present work, characterisation of the material at the first stage of production as melt-spun ribbon and flake has been carried out. The microstructures show typical characteristics of a 'featureless zone' on the wheel-side and coarser microstructures on the air-side, with clusters of silicon particles evident. At high magnification, on the wheel-side, TEM and FEGSEM reveal local variations in the silicon and aluminium content (although on average there is no macrosegregation from the wheel-side to the air-side during solidification). In FEGSEM, the 'rosette-structure' also displays local variations in Al, Si, Fe, Cu and Ni over a scale of a few microns.

Introduction

Specific qualities of materials such as resistance to corrosion, resistance to wear, specific strength and ability to withstand high temperatures are of great advantage in the automotive industry. Aluminium silicon alloys have proven to be exceptional due to corrosion resistance, low wear rates and low thermal expansion. Aluminium is widely used in the automotive industry because of its low density ($2.7g/cm^3$), an advantage to weight reduction and gas mileage. These properties have become ideal in the production of a variety of automotive parts such as pistons, connecting rods and many more. Silicon is one of the elements which when added to aluminium has minimum weight increment (Si density $2.33g/cm^3$). Increase in silicon in aluminium-silicon alloys results in increase in the wear resistance and mechanical properties as long as the Si content is below eutectic range [1, 2]. However, increasing silicon content beyond the eutectic composition causes the formation of large silicon particles which affect the toughness of the alloy. There is a drive to increase the silicon content well into the hypereutectic range because of the low thermal expansion coefficient, high specific stiffness and strength, good hot strength and excellent wear resistance. Rapid solidification processing is a technique used for refining the primary silicon and seems to be the most promising technique for the production of high Si Al-Si alloys (i.e. Si content greater than 17 wt. %).

There are number of routes which can be used to produce rapid solidification, including spray methods, weld methods, and chill methods. Of these, melt spinning is the most widely used industrially due to its high cooling rate and the ability to process large volumes of materials. The material for this paper was supplied by RSP Company in The Netherlands, who use melt spinning to produce rapid solidification.   Flakes are produced by chopping melt spun ribbon and are then either 'free encapsulated' (i.e. placed in a canister without compaction prior to degassing) or consolidated (i.e. cold precompacted to 60% theoretical density) before degassing. The canister is then sealed and hot isostatically pressed to full (or almost full) density. The capsule is machined off, to avoid the mixing of aluminium with Al-Si material, and the billet extruded. Here we focus on characterising the material in its melt spun condition, as ribbon or flake, as a precursor to investigating the later stages in the processing.

Rimental Details

Materials. The two alloys examined here are denoted 431 and 461 by RSP. 431 has composition (wt%) 29.8 Si, 1.3 Cu, 1.4 Mg, 0.3 Fe, 0.3 Ni, 0.3 Zr (balance Al). 461 has composition 21 Si, 3.9 Cu, 1.2 Mg, 2.4 Fe, 1.4 Ni, 0.4 Zr (balance Al). Essentially, 431 is a relatively high Si alloy with low Cu, Fe, Ni and 461 a relatively low Si alloy (but still with 21wt% Si) and high Cu, Fe, Ni. The materials were supplied as either ribbon or flake. The material supplier provided the compositions which were obtained by chemical dissolution, Si determination via gravimetry and determination of metallic elements by XRF using borate fusion, standard DIN ISO 4503. The flake average thickness is 40 μm, the length is 1.4 mm, and width is 1.2 mm. Ribbon average thickness is 40 μm, and width is 2.5 mm. This suggests the ribbons have split lengthways during chopping to form the flakes.

Optical Metallography. Two to three flakes or ribbons from each flake or ribbon batch supplied by RSP were placed in a plastic clip to hold them in such a way that transverse sections could be obtained. Samples were hot mounted. Mounting was conducted in a Struers LaboPress-3 with a cure temperature of $180^{\circ}C$ and a mounting pressure of 15kN. Samples were then ground and polished using a Buehler Metaserv polishing machine. Grinding operations used SiC paper of 240, 400, 600, 800, 1000 and 2500 grit, followed by polishing with 6μm and 3 μm, and a final polish with colloidal silica Dp-Com. Grinding and polishing times was one minute for each stage. The grinding liquid was water. Polishing liquids were propanol plus water and 6-micron diamond was used for 6 μm polishing. Struers oil-based lubricating liquid was used for diamond polishing; 3-micron diamond was used for 3 μm polishing and aqueous solution of 0.1 μm colloidal SiO_2 was used for colloidal silica polishing. After each grinding stage, specimens were then washed with water and soap. Then, after each polishing stage, specimens were cleaned using a Struers Ultrasonic bath for 2 minutes to remove any dirt or particles remaining on the polished surface. Specimens were washed with water and soap. Finally, they were washed with alcohol to remove any final dirt and water residue. Specimens were then hot dried. Optical microscopy was conducted using an Olympus Vanox.

Field Emission Gun Scanning Electron Microscopy (FEGSEM). Field emission gun scanning electron microscopy (FEGSEM) was conducted using an FEI Sirion 200 FEGSEM. The operating voltage used was 20kV and the working distance was 5 mm. Both backscattered and secondary electron techniques were used. Quantitative analysis was carried out to determine the chemical composition of each sample with Energy Dispersive X-Ray Analysis Princeton Gamma Technology Avalon (EDX).

Transmission Electron Microscopy (TEM). Transmission electron microscopy (TEM) was carried out using a JEM-2100 LaB$_6$ TEM at 200keV and fitted with a PGT Energy Dispersive X-ray analysis system (EDX). The ribbon samples had a thickness of 40 μm and further mechanical reduction was impossible to achieve due to the brittleness of the material. Thin foil samples were prepared in the Precision Ion Polishing System (PIPS) using argon ions at an energy of 3-5 keV. The bombardment angles were first set at 4° for 1hr, and reduced to a smaller angle of 3° to finish until penetration was visible. The time required was 2 hrs.

Experimental Results and Discussion

Fig. 1 shows an optical micrograph of the microstructure of 431 flake and 461 ribbon. Fig.1 (a) shows the air-side microstructure (the material immediately adjacent to the wheel is termed 'wheel-side') which consists of fine silicon particles uniformly distributed throughout the aluminium matrix. Some cracks through silicon particles are visible, which may have occurred due to the thermal gradient during the rapid solidification, during the chopping process, or just possibly during specimen preparation. Fig. 1 (b) reveals two zones: a featureless zone (Zone 1) and a coarse Si-particle zone (Zone 2). The highest cooling and solidification rates occur at the wheel-side (the featureless zone) which is usually characterised by a straight line rather than the wavier surface of the air-side. The chilling effect usually leads to very small crystallites in this region, or potentially an amorphous structure. The microstructure is consistent with that obtained by other workers [3-14]. The wheel side with the relatively featureless zone can also be seen in Fig. 2, which is a

FEGSEM backscattered micrograph for 461 ribbon. The microstructure for the air-side is coarser than that for the wheel-side. Comparing average widths for flakes with those for ribbons suggests that ribbons tend to split lengthways during the chopping process. This then means (with reference to Fig. 1 (b)) that some flakes tend to have the 'featureless' type microstructure before further processing, whilst other exhibit the coarser air-side type microstructure.

(a)

(1) Cracking
(2) Clusters of silicon
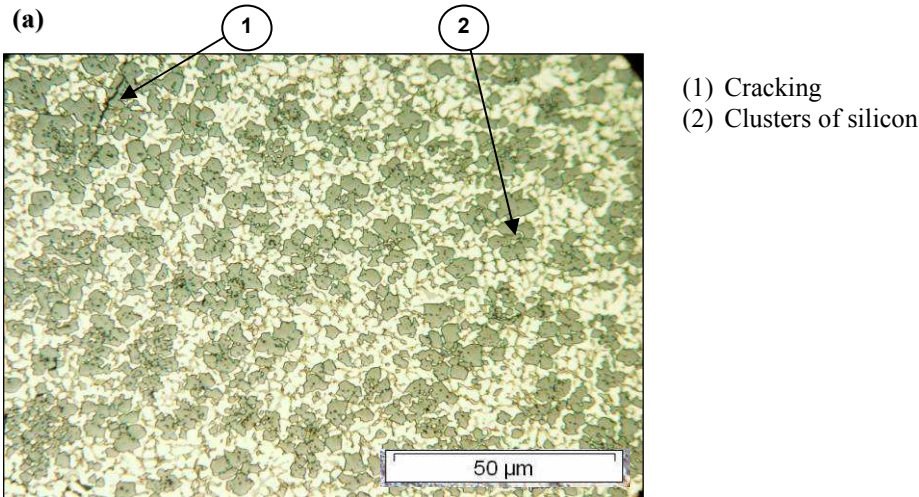
Fig. 1 (a) 431 alloy (Al 29.8Si 1.3Cu 1.4Mg 0.3Fe 0.3Ni 0.3Zr) flake optical micrograph etched, air side longitudinal cross-section, (b) 461 ribbon (Al 21Si 3.9Cu 1.2Mg 2.4Fe 1.4Ni 0.4Zr) optical micrograph longitudinal section.

(b)

(1) Zone 1
(2) Zone 2
(3) Wheel side
(4) Mount
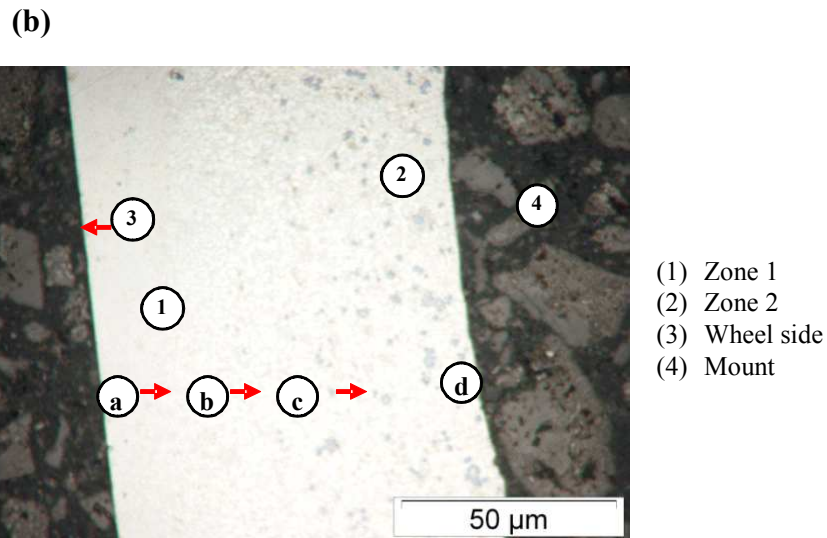
Fig. 2 FEGSEM backscattered micrograph of 461 ribbon (Al 21Si 3.9Cu 1.2Mg 2.4Fe 1.4Ni 0.4Zr) unetched.
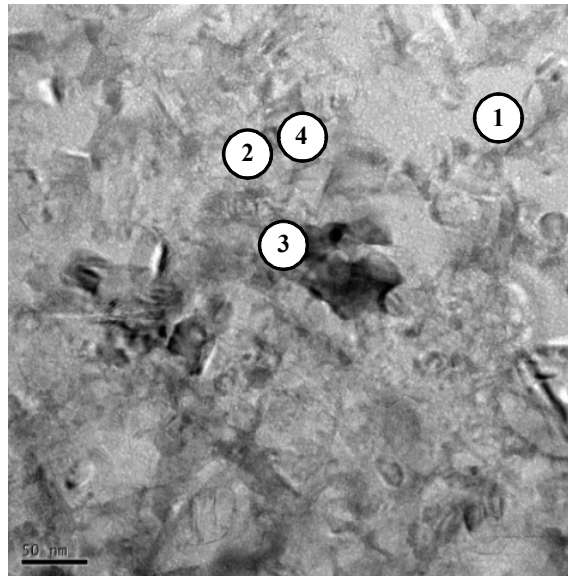
Fig. 3 TEM micrograph of 461 (Al 21Si 3.9Cu 1.2Mg 2.4Fe 1.4Ni 0.4Zr) ribbon unetched. Points 1,2,3,4 and 2 were analysed by EDX (see Fig. 4)
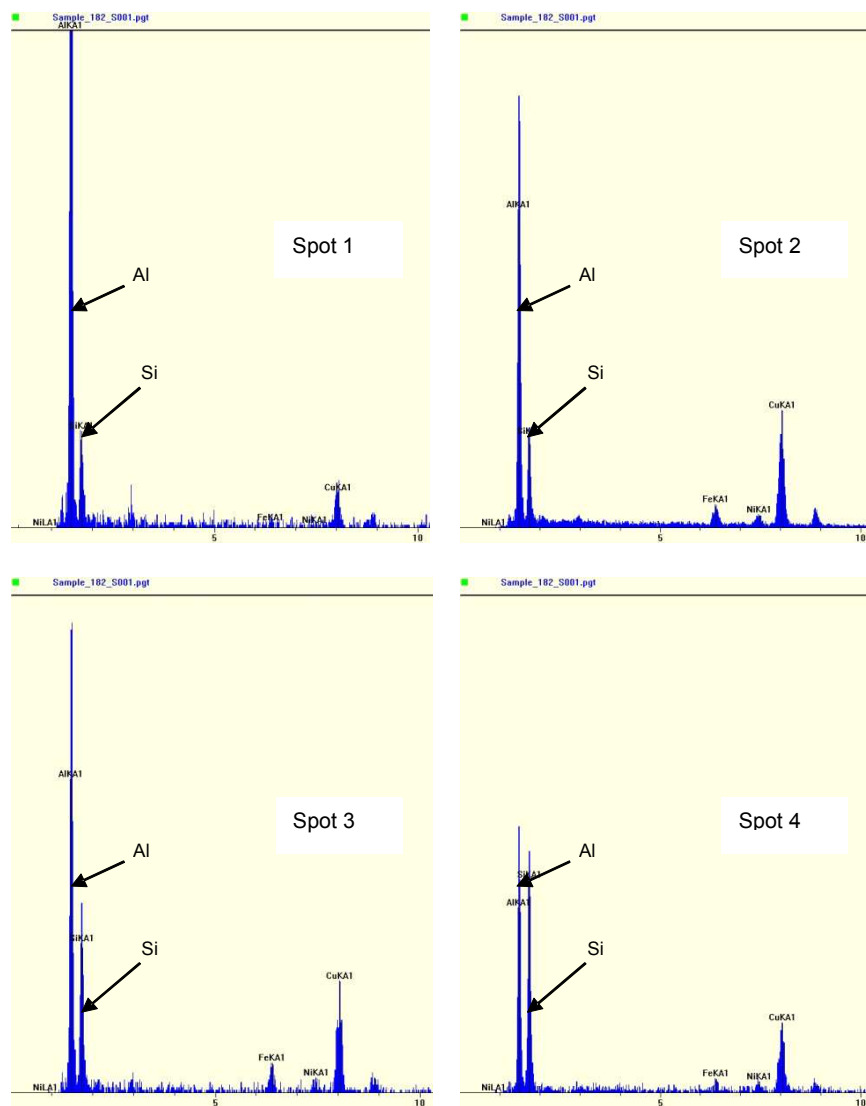
Fig. 4 EDX spectra for points 1. 2. 3 and 4 in Fig. 3, showing relatively high Al in points 1 and 2 and relatively higher Si for points 3 and 4.

(a) (b)
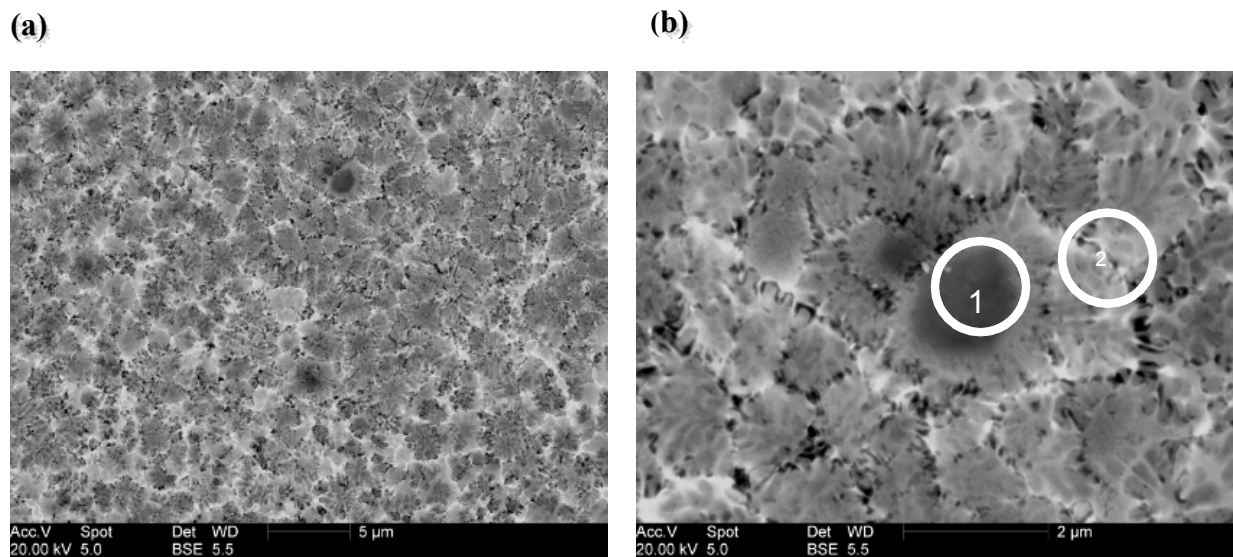
Fig. 5 FEGSEM backscattered electron micrographs of 461 (Al 21Si 3.9Cu 1.2Mg 2.4Fe 1.4Ni 0.4Zr) ribbon.

Fig. 3 shows a TEM micrograph of the ribbon sample 461. Four different points are indicated. EDX spectra for these are shown in Fig. 4. Points 1 and 2, which are relatively pale on the micrograph, have relatively high content of aluminium and points 3 and 4, which appear dark on the micrograph, have a relatively higher content of silicon. The distances between these points are a few tens of nm. FEGSEM micrographs of the 461 ribbon about 20 microns from the wheel-side (i.e. at the transition between the featureless zone and the zone with features in Fig. 2) are shown in Fig. 5. The microstructure shows rosette like morphology, consistent with the literature on rapid solidification [4,14,15]. Point number one on Fig. 5 (b), which appears dark grey on the micrograph, has a relatively high content of Si and point number two, which appears pale, has a relatively high content of Al. The difference in contrast in the backscattered micrograph must be due to the difference in the composition in terms of Fe, Ni and Cu, since these elements are heavier than Al and Si which have very similar atomic numbers.

When quantitative EDX analysis is carried out on areas across the cross-section from the wheel-side to the air-side, there is little evidence for segregation from the wheel side towards the air side during solidification.

Undercooling of the molten metal occurs due to the high cooling rate. The solidification of this sample can be explained using Fig. 6. With slow cooling of an Al-20%Si alloy, at 'a' the alloy is liquid. As the alloy cools, solid Si starts to form at 'b'. With further decrease of temperature, at 'c' the remaining liquid becomes eutectic. With fast cooling (but not so fast) the liquid is quenched to an amorphous structure of the same composition; little diffusion can take place. It is as though the liquidus and solidus from the left hand side are extended. At 'b', solid Si does form, and at 'c' eutectic, but at 'd' some alpha aluminium will also be present and this can be seen in Fig. 1 (a). This is not an equilibrium phase in an Al-20%Si alloy so will only be present under rapid solidification conditions.
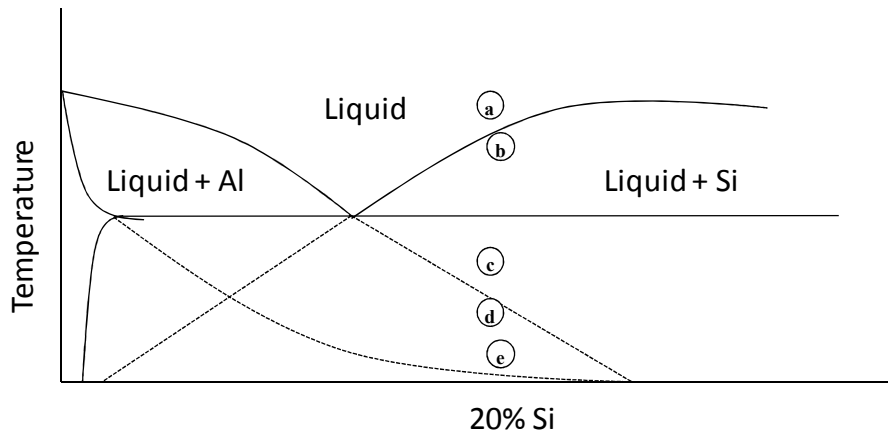
Fig. 6 The solidification of sample

Summary and Conclusions

Flake and ribbon microstructures of as-received melt spun samples have been obtained using optical microscopy, FEGSEM and TEM. The microstructures show typical characteristics of a 'featureless zone' on the wheel-side and coarser microstructures on the air-side, with clusters of silicon particles evident. At high magnification, on the wheel-side, TEM and FEGSEM reveal local variations in the silicon and aluminium content (although on average there is no macrosegregation from the wheel-side to the air-side during solidification). In FEGSEM, the 'rosette-structure' also displays local variations in Al, Si, Fe, Cu and Ni over a scale of a few microns. The evidence from measuring the width of flakes (which are used in subsequent processing of rapidly solidified alloy), is that the ribbons tend to split lengthways during chopping so that some flakes have the microstructure characteristic of the 'wheel-side' with the featureless zone and some of the air-side with the coarser structure.

Acknowledgments

References

[1] " Metals Handbook, Properties and Selection: Nonferrous Alloys and Special-Purpose Materials ", 10th ed. vol. 2: ASM, Metals Park, Ohio, 1990, p. 124.

[2] F. J. Dom, "Meltspun Aluminium Successful in Racing Piston," Aluminium, vol. 70, pp. 575-578, 1994.

[3] R. Dasgupta, "Property Improvement in Al-Si Alloys through Rapid Solidification Processing," Journal of Materials Processing Technology, vol. 72, pp. 380-384, 1997.

[4] N. Unlu, A. Genc, M. L. Ovecoglu, N. Eruslu, and F. H. Froes, "Characterization Investigations of Melt Spun Ternary Al-xSi-3.3Fe (x=10, 20 wt.%) Alloys," Journal of Alloys and Compounds, vol. 322, pp. 249-256, 2001.

[5] L. Yuan-yuan, Z. Da-tong, N. Leo, and Z. Wei-wen, "Rapidly Solidified Hypereutectic Al-Si Alloys Prepared by Powder Hot Extrusion," Transaction Nonferrous Metals Soc. China, vol. 12, pp. 878-881, 2002.

[6] M. V. Rooyen, P. F. Colijn, T. H. Keijser, and E. J. Mittemeijer, "Morphology and Mechanical Properties of Melt-Spun and Conventionally Cast Aluminium, AlMg and AlSi Alloys Before and after Hot Extrusion," Journal of Materials Science vol. 21, pp. 2373-2384, 1986.

[7] H. H. Liebermann, "Rapidly Solidified Alloys Made by Chill Block Melt Spinning Processes," Journal of Crystal Growth, vol. 70, pp. 497-506, 1984.

[8] P. Todeschini, G. Champier, and F. H. Samuel, "Production of Al-(12-25) wt% Si Alloys By Rapid Solidification: Melt Spinning Versus Centrifugal Atomization," Journal of Materials Science, vol. 27, pp. 3539-3551, 1992.

[9] C. Antonione, L. Battezzati, and F. Marino, "Structure and Stability of Rapidly Solidified Al-Si base Alloys," Journal of Materials Science Letters, vol. 5, pp. 586-588, 1986.

[10] O. Uzun, T. Karaaslan, and M. Keskin, "Production and Structure of Rapidly Solidified Al-Si Alloys," Turk Journal of Physics, vol. 25, pp. 455-466, 2001.

[11] R. Delhez, T. Keijser, E. Mittemeijer, P. Mourik, N. Pers, L. Katgerman, and W. Zalm, "Structural Inhomogeneties of AlSi Alloys Repidly Quenched from the Melt," Journal of Materials Science, vol. 17, pp. 2887-2894, 1982.

[12] C. Rios, S. Santos, W. Botta, C. Bolfarini, and C. Kiminami, "Microstructural Characterization of As-quenched and Heat treated Al-Si-Mg Melt Spun Ribbons," Journal of Metastable and Nanocrystalline Materials, vol. 22, pp. 103-108, 2004.

[13] C. Sivaramakrishnan, K. Lala, and R. Mahanti, "Characterizationof Rapidly Solidified Structures of Al-6Fe-3MM," Journal of Materials Science, vol. 26, pp. 4369-4374, 1991.

[14] V. C. Srivastava, P. Ghsal, and S. N. Ojha, "Microstructure and Phase Formation in Spray Deposited Al-18%Si-5%Fe-1.5%Cu Alloy," Materials Letters, vol. 56, pp. 797-801, 2002.

[15] D. M. Wilkes and H. Jones, "Structure and Properties of Rapidly Solidified Al Rich Al-Mn-si Alloys," Journal of Materials Science, vol. 34, pp. 735-747, 1999.

Mechatronics and Materials Processing I

10.4028/www.scientific.net/AMR.328-330

Microstructural Characterization of Rapidly Solidified Al-High Si Alloys

10.4028/www.scientific.net/AMR.328-330.1545